Title

Astrocyte-derived extracellular vesicles enhance the survival and electrophysiological function of human cortical neurons in vitro.

Authors

Chun, Changho
Smith, Alec
Kim, Hyejin
et al.

Publication Date

2021-04-01

DOI

10.1016/j.biomaterials.2021.120700

Peer reviewed

HHS Public Access

Author manuscript

Biomaterials. Author manuscript; available in PMC 2022 April 01.

Published in final edited form as:

Biomaterials. 2021 April ; 271: 120700. doi:10.1016/j.biomaterials.2021.120700.

Astrocyte-derived Extracellular Vesicles Enhance the Survival and Electrophysiological Function of Human Cortical Neurons *in vitro*

Changho Chun[1,§], **Alec S.T. Smith**[2,7,§], **Hyejin Kim**[3], **Dana S. Kamenz**[1], **Jung Hyun Lee**[2,8], **Jong Bum Lee**[3], **David L. Mack**[1,2,6], **Mark Bothwell**[2,7], **Claire D. Clelland**[4,5], **Deok-Ho Kim**[1,2,9,10,11,12,*]

[1]Department of Bioengineering, University of Washington, Seattle, WA 98195, USA

[2]Institute for Stem Cell and Regenerative Medicine, University of Washington, Seattle, WA 98109, USA

[3]Department of Chemical Engineering, University of Seoul, Seoul, South Korea

[4]Gladstone Institute, San Francisco, CA 94158, USA

[5]Department of Neurology, University of California San Francisco, San Francisco, CA 94143, USA

[6]Department of Rehabilitation Medicine, University of Washington, Seattle, WA 98195, USA

[7]Department of Physiology & Biophysics, University of Washington, Seattle, WA 98195, USA

[8]Division of Dermatology, School of Medicine, University of Washington, Seattle, WA 98195, USA

[9]Department of Biomedical Engineering, Johns Hopkins University, Baltimore, MD 21205, USA

[10]Department of Medicine, Johns Hopkins School of Medicine, Baltimore, MD 21205, USA

[11]Department of Neurology, Johns Hopkins School of Medicine, Baltimore, MD 21205, USA

[*]To whom correspondence should be addressed: Dr. Deok-Ho Kim, Associate Professor, Department of Biomedical Engineering, The Johns Hopkins University School of Medicine, Ross Research Building, 715B, 720 Rutland Avenue, Baltimore, MD 21205, dhkim@jhu.edu.

CRediT Author Statement

Changho Chun: Conceptualization, Astrocyte culture, EV collection and characterization, all of the data analysis, manuscript draft preparation

Alec S.T. Smith: Patch-clamp experiment, manuscript proofreading

Hyejin Kim: Additional EV characterization experiment

Dana S. Kamenz: EV collection

Jung Hyun Lee: Flow cytometry experiment

Jong Bum Lee: Support Hyejin's experiment, financial support

David L. Mack: Data analysis, manuscript proofreading

Mark Bothwell: Conceptualization, manuscript proofreading

Clair D. Clelland: iPSC culture

[§]These authors contributed equally to this work.

Declaration of interests

☒ The authors declare that they have no known competing financial interests or personal relationships that could have appeared to influence the work reported in this paper.

[12]Department of Physical Medicine and Rehabilitation, Johns Hopkins School of Medicine, Baltimore, MD 21205, USA

Abstract

Neurons derived from human induced pluripotent stem cells (hiPSCs) are powerful tools for modeling neural pathophysiology and preclinical efficacy/toxicity screening of novel therapeutic compounds. However, human neurons cultured *in vitro* typically do not fully recapitulate the physiology of the human nervous system, especially in terms of exhibiting morphological maturation, longevity, and electrochemical signaling ability comparable to that of adult human neurons. In this study, we investigated the potential for astrocyte-derived extracellular vesicles (EVs) to modulate survival and electrophysiological function of human neurons *in vitro*. Specifically, we demonstrate that EVs obtained from human astrocytes promote enhanced single cell electrophysiological function and anti-apoptotic behavior in a homogeneous population of human iPSC-derived cortical neurons. Furthermore, EV-proteomic analysis was performed to identify cargo proteins with the potential to promote the physiological enhancement observed. EV cargos were found to include neuroprotective proteins such as heat shock proteins, alpha-synuclein, and lipoprotein receptor-related protein 1 (LRP1), as well as apolipoprotein E (APOE), which negatively regulates neuronal apoptosis, and a peroxidasin homolog that supports neuronal oxidative stress management. Proteins that positively regulate neuronal excitability and synaptic development were also detected, such as potassium channel tetramerization domain containing 12 (KCTD12), glucose-6- phosphate dehydrogenase (G6PD), kinesin family member 5B (KIF5B), spectrin-alpha non-erythrocytic1 (SPTAN1). The remarkable improvements in electrophysiological function and evident inhibition of apoptotic signaling in cultured neurons exposed to these cargos may hold significance for improving preclinical *in vitro* screening modalities. In addition, our collected data highlight the potential for EV-based therapeutics as a potential class of future clinical treatment for tackling inveterate central and peripheral neuropathies.

Keywords

Extracellular vesicles; human cortical neuron; astrocyte; electrophysiology; survival

1. Introduction

The mammalian cerebral cortex is well organized with specific layers supporting distinct neuronal populations.[1–3] Within the cortex, neurons not only form connections with each other, but also with supporting glial cells. These neuroglial interactions are indispensable for ensuring neuron survival, differentiation, maturation, regeneration and proper coordination of motor and sensory information in the brain.[3–8] Astrocytes are the most abundant subtype of glial cells coexisting with neurons in the central nervous system (CNS). They are known to provide structural and trophic support to neurons, mediate synaptogenesis at early stages of neonatal brain development, maintain and eliminate neuronal synapses, and modulate excitability of associated neurons.[9] Animal studies have revealed that astrogenesis, which begins during the later stages of neurogenesis (around E18 in rodents), coincides with axon and dendrite outgrowth as well as synaptic initiation in neurons.[9,10] Although numerous

studies have revealed a diverse range of astrocyte functionality on neurons, detailed mechanisms of how these nerve cells specifically interact with each other during development and beyond, and how their interactions are altered in diseased tissues, are not well understood. Recent studies using murine-derived cells have described EV-mediated neuronal modulation by astrocytes in response to inflammatory or oxidative stress[11–15], or from genetic mutation causing neurodegenerative disease.[16,17] These studies have significantly broadened our understanding of exosome-mediated control of neurons by astrocytes in pathologic conditions, but we still lack critical information on how astrocyte-derived EVs modulate neuronal physiology in the normal human nervous system. Given that astrocytes show species-specific characteristics to exhibit significantly varied physiological features in different organisms, reliable human model study of EV-mediated astrocyte-neuron interactions will highly contribute to understanding neuroglial communication in normal human CNS development.

In this study, we utilized hiPSC-derived cortical neurons and human astrocyte-derived EVs to investigate the effect of EVs on the physiological behavior of human neurons, with a particular focus on their positive regulation of neuronal survival and electrophysiology. The data presented here highlight the neuroprotective role of astrocyte-derived EVs, as evidenced by reduced apoptotic signal expression and enhanced electrophysiological function in treated neurons. In addition, we analyzed the proteomic profile of astrocyte EVs in order to identify cargo molecules that may be responsible for the observed enhancement of neuronal survival and function.

2. Materials and Methods

2.1. Astrocyte cell culture

Commercially sourced human primary astrocytes were purchased from ScienCell Research Laboratories (Carlsbad, CA) and were stored, thawed and sub-cultured based on the manufacturer's protocol. Cultures were maintained in a 37 °C / 5 % CO_2 incubator throughout the culture period and the astrocytes were used up to passage five, to maintain consistent cell quality. Initially, the astrocytes were cultured for 72 hours in a base medium with an astrocyte growth supplement and fetal bovine serum provided by the same manufacturer. After 72 hours of culture, the medium was replaced with an EV-free medium consisting of the base medium plus EV-depleted serum and supplement. The cells were then cultured for an additional 12 to 84 hours, allowing them to secrete a maximal number of EVs, while maintaining less than 90% cell confluency before collection of the conditioned medium.

2.2. Human iPSC maintenance and cortical neuron differentiation

WTC11 human induced pluripotent stem cells stably transduced with a doxycycline-mediated Ngn-2 overexpressing transgene were kindly provided by the Gladstone Institute (San Francisco, CA). These cells were maintained and differentiated according to the Gladstone protocol published previously.[18,19]

The hiPSCs were differentiated into human cortical neurons using a previously reported method with limited modifications. Specifically, 80% confluent hiPSC colonies on Matrigel-coated plates (Corning) were dissociated into single cells using Accutase (Thermo-Fisher) and transferred on to fresh Matrigel-coated plates. The cells were then treated with an induction medium including N2 supplement (100x, Thermo-Fisher), non-essential amino acids (100x, Thermo-Fisher), Glutamax (100x, Thermo-Fisher) and doxycycline (1000x, Sigma-Aldrich) to initiate differentiation. The cultures were maintained with the same induction medium replenished every day for 48 hours before being passaged and transferred to the final assay plate. Differentiated neurons at day 3 post-induction were transferred to 0.01% poly-L-ornithine (Sigma-Aldrich) and 5 μg/mL laminin (Sigma-Aldrich) coated glass coverslips for subsequent analysis. Cells were then fed with BrainPhys medium supplemented with B27 (Invitrogen), laminin (Sigma-Aldrich), and 10 ng/mL brain derived neurotrophic factor (BDNF; R&D Systems) every 3 days until endpoint analysis.

2.3. EV isolation and characterization

Astrocytes were cultured with vendor-provided base medium supplemented with EV-depleted serum. The culture medium in which cell-derived EVs were secreted was collected after 12, 24, 36, 48, or 84 hours of culture. A multi-step ultracentrifugation protocol was then applied to concentrate and purify the EVs. First, a spin at 300 rcf for 10 minutes was used to remove detached cells. 2,000 rcf for 10 minutes was then used to remove dead cells before a spin at 10,000 rcf for 30 minutes was applied to remove cell debris and apoptotic bodies. The EVs were then collected following 2 repeated ultracentrifugation steps at 30,000 rcf for 70 minutes. The EVs in the final solution were sterile filtered using a 0.2 μm filter, resuspended in 50 μL of BrainPhys medium (Stem cell technologies), and stored at −80 °C for up to one month until use. The size distribution and density of the collected EVs were analyzed using a Nanoparticle Tracking Analyzer (Nanosight of Malvern Institute). Storage temperature-dependent changes in modal size and particle concentration were analyzed at different temperatures (4 °C, −20 °C and −80 °C) at day 3 and 7. The changes in physical properties and total protein concentration of EVs after repeated freeze-thawing cycles was analyzed using isolated EVs that were repeatedly incubated at −80 °C and thawed at room temperature. After each cycle, EV proteins were quantified using the Micro BCA Protein Assay Kit (Thermo Fisher) and following the manufacturer's protocol. The modal size and particle concentrations were measure using Nanoparticle Tracking Analyzer.

2.4. TEM imaging

For transmission electron microscopy imaging of EVs, a Titan TM 80–300 (FEI) was employed at an accelerated voltage of 200 kV. The isolated EVs were resuspended in DPBS and the samples were deposited onto a Lacey Formvar/carbon-coated copper grids, then air-dried at room temperature before analysis.

2.5. Immunocytochemistry

To verify successful differentiation of cortical neurons and homogeneity of cultured astrocytes, cells were immunostained for expression of cortical neuron (layer 2 and 3) and glia specific markers. Briefly, cells were fixed in 4% paraformaldehyde for 15 minutes followed by permeabilization using 0.2% triton-X solution for 10 minutes. Cells were then

blocked with 0.5% BSA in PBS for 1 hour at room temperature. After blocking, cells were incubated with primary antibodies diluted in 0.5% BSA solution in PBS overnight at 4°C. The next day, cells were washed 3 times with PBS, and incubated for 2 hours in a secondary antibody solution containing secondary antibodies diluted in 0.5% BSA solution in PBS. Coverslips were mounted on microscope slides using Vectashield containing DAPI (Vector Labs) to counterstain samples for nuclei. Images were taken at the Garvey Imaging Core at the University of Washington's Institute for Stem Cell and Regenerative Medicine using a Nikon A1 Confocal System on a Ti-E inverted microscope platform. Antibodies used in these experiments were as follows: rabbit anti-MAP-2 (1:1000, Millipore), mouse anti-CUX-1(1:500, Thermo-Fisher), chicken anti-GFAP (1:1000, Invitrogen), mouse anti-S100B (1:500, Sigma-Aldrich), Alexafluor-594 conjugated goat-anti-mouse secondary antibody (1:500, Invitrogen), Alexafluor-594 conjugated goat-anti-chicken secondary antibody (1:500, Invitrogen) Alexafluor-488 conjugated goat-anti-mouse secondary antibody (1:500, Invitrogen) and Alexafluor-647 conjugated goat-anti-rabbit secondary antibody (1:200, Invitrogen).

2.6. EV labeling and uptake study

An ExoGlow-protein EV labeling kit (System Biosciences, Palo Alto, CA) was used for live cell EV imaging. Collected EVs were incubated for 20 minutes with the labeling dye (1:500) at 37 °C to induce vesicular protein conjugation with the dye molecules. Then the solution was treated with the ExoQuick-TC solution and incubated for 2 hours at 4 °C, followed by centrifugation at 10,000 rcf for 10 minutes to remove unlabeled reagent molecules and collect labeled EVs only. The labeled EVs were resuspended in neuronal maintenance medium and added to neurons 72 hours post-differentiation at various concentrations. A live cell imaging microscope (Eclipse T1, Nikon) was used to image fluorescently labeled EV uptake by the cultured neurons. In these experiments, images were collected at multiple locations from examined culture wells every 5 minutes for 2 hours. Additionally, neurons treated with unlabeled EVs were fixed after 2 hours of treatment and immunostained with a mouse anti-CD81 antibody (1:100, Thermo-Fisher) to quantify the relative amount of internalized EVs based on fluorescence intensity. CD81 labeling was coupled with fluorescently-labelled phalloidin (for F-actin visualization; 1:200, Invitrogen) to confirm the correct positioning of CD81 expression relative to the cell cytoskeleton.

2.7. Cell senescence and apoptosis assay

To quantify the population of senescent neurons in each culture condition, a β-galactosidase staining kit (Sigma-Aldrich) was used. The cells were fixed at day 4 with 4% paraformaldehyde (PFA) for 15 minutes. The staining solution was prepared by mixing 25 μL of the X-gal solution with 475 μL of iron buffer to make a total of 500 μL for each well. The staining solution was added to the culture and kept at 37 °C for 3 hours before assessment. The number of cells exhibiting blue dye accumulation in their cytoplasm under bright field microscope was then compared for each group. To quantify apoptotic cells in these cultures, Annexin 5 (Thermo-Fisher) with propidium iodide (PI, Thermo-Fisher) was used to label cells for flow cytometry analysis (BD Canto II). Specifically, 200,000 cells per condition were treated with fluorescently labelled Annexin V and propidium iodide for 15 minutes at room temperature. These cells were then immediately washed before flow

cytometry analysis to minimize cell death during the assay process. The number of cells expressing Annexin V and/or PI in each group was then analyzed and quantified using FlowJo software (BD Biosciences).

2.8. Morphological assessment of neurons

To examine the effect of astrocyte-derived EV treatment on axon outgrowth, cultured neurons were imaged 2 hours, 6 hours and 12 hours after plating. The length of the longest neurite segment for each neuron was measured for every image taken at each time point. Additionally, neurons from each group were fixed at each timepoint and stained with anti-neurofilament to enable comparative assessment of axon length. The axon morphologies were analyzed using the Simple Neurite Tracer plugin in ImageJ. To measure axon branching, the neurons immunostained for neurofilament expression were individually analyzed using the NeuronJ plugin for ImageJ to identify the divergence of axon terminals.

2.9. Electrophysiological assessment of neurons

Electrophysiological function of neurons in each group was recorded using whole-cell patch clamp techniques. Recordings were performed on an inverted DIC microscope (Nikon) connected to an EPC10 patch clamp amplifier and computer running Patchmaster software (HEKA). Coverslips supporting cultured neurons were loaded onto the microscope stage and bathed in a Tyrode's solution containing 140 mM NaCl, 5.4 mM KCl, 1.8 mM $CaCl_2$, 1 mM $MgCl_2$, 10 mM glucose, and 10 mM HEPES. The intracellular recording solution (120 mM L-aspartic acid, 20 mM KCl, 5 mM NaCl, 1 mM $MgCl_2$, 3 mM Mg^{2+}-ATP, 5 mM EGTA, and 10 mM HEPES) was loaded into borosilicate glass patch pipettes (World Precision Instruments) with a resistance in the range of 2–6 MΩ. Offset potentials were nulled before formation of a gigaΩ seal. Suction was then applied to disrupt the cell membrane in contact with pipette end. This process allowed electrical and molecular access to the intracellular space, and membrane potentials were then corrected by subtraction of the liquid junction potential, calculated by Patchmaster. The current clamp mode was used for recording action potential behavior of neurons. Specifically, a 2 nA depolarizing single pulse was applied for 5 ms to induce single action potentials, and stepwise current injections of 10 pA from −30 to +70 pA for 500 ms were applied to trigger repetitive action potential firing. The action potential duration at 90% repolarization (APD90), depolarization speed and repolarization speed were recorded for each group of neurons by the Patchmaster software. Inward and outward currents were evoked in voltage clamp mode, by providing 500 ms depolarizing steps from −120mV to +30mV in 10 mV increments. To measure resting membrane potential of neurons in each group, gap-free recordings of spontaneous activity in patched neurons were performed in current-clamp mode with 0 pA current injection. The analyses of action potential waveforms and currents were performed using the Patchmaster software suite. All reagents used in this protocol were obtained from Sigma-Aldrich.

2.10. Proteomics analysis

The protein cargo profile of astrocyte-derived EVs was analyzed using a commercial proteomics service (System Biosciences). Astrocyte conditioned medium was sampled after 84 hours of culture for EV collection followed by protein isolation and mass spectrometry.

Raw data was analyzed using Proteome Discoverer (Thermo-Fisher). Protein function was then evaluated using the gene ontology browser DAVID (version 6.8).

2.11. Statistical analysis

All experiments were performed using at least 3 independently cultured neuron populations. EV treatments were derived from 4 independent batches of cultured astrocytes. Significant differences between groups were evaluated using either unpaired, two-tailed t-tests or Mann Whiney-U tests depending on whether the data was normally distributed. One-way analysis of variance (ANOVA), or ANOVA on ranks depending on data normality, with *post hoc* tests for multiple comparisons were used to compare data sets with more than two experimental groups. For analysis of repetitive firing via patch clamp, contingency tables were constructed and used to run chi squared tests to determine whether the distribution of data was dependent on cell type. In all experiments, a p value of less than 0.05 was considered significant. All statistical tests were performed using the GraphPad Prism statistics software (GraphPad Software Inc.).

3. Results

3.1. Doxycycline-mediated overexpression of Neurogenin-2 is sufficient to drive cortical neuron differentiation from hiPSCs

Human cortical neurons were obtained following the previously developed protocol that uses an iPSC line harboring a doxycycline-inducible neurogenin-2 (Ngn2) transgene; a transcription factor that drives rapid conversion of stem cells to neurons.[19] Briefly, neuronal differentiation was induced by applying doxycycline for 24 hours after single cell dissociation of iPSCs and completed by exposing the early stage neurons to a specific induction medium for an additional 48 hours. This was then followed by a change to medium supplemented with BDNF, B27, and laminin from day 3 onwards (Figure 1A). In the first 24-hour period following induction, stem cells rapidly became polarized and began to exhibit growth cones indicative of initial neurite outgrowth. By day 3, neurite growth was more apparent and distinct axon outgrowth in each cell was observed. Cells at day 7 gained a typical neuronal morphology characterized by long axons with branched dendrites approaching those of adjacent cells and small, well-defined soma (Figure 1B). Differentiated neurons were transferred to laminin-coated assay plates at day 3 for further maturation and analysis. The overall differentiation period (3 days) was dramatically shorter than that required in conventional human iPSC-derived neuron differentiation, which can take 4–6 weeks.[7,20,21] Immunocytochemistry data collected from these cells demonstrated a high degree of homogeneity of cortical neurons for each experimental batch (n = 5), indicating significant enhancements in reproducibility and yield, compared to conventional, small molecule-mediated differentiation of human neurons. In particular, the uniform expression of CUT-like homeobox 1 (CUX-1) observed in the majority of examined cells verified the successful generation of pyramidal cortical neurons specific to upper layers of the cerebral cortex. The immunocytochemistry results highlight the reliability of the described method for producing differentiated neurons with which to study the effect of internalized EVs (Figure 1C).

3.2. Ultracentrifugation of human astrocyte conditioned medium leads to isolation of consistent and highly-uniform EVs

The homogeneity of the cultured astrocyte population was confirmed using immunostaining for two glial cell-specific protein markers, GFAP and S100B, which are known to be primarily expressed in the astrocyte cytoplasm (Figure 2A, 2B). Astrocyte-EVs were collected by serial ultracentrifugation (Figure S1). TEM images of negative stained EVs (Figure 2C) and the Brownian motion observed from laser-scattered particles in the assay solution (Supplementary video S1) demonstrate the successful isolation of EVs from the conditioned medium. The mean mode size of collected EVs was 124 nm, with a density of 1.5×10^9 particles/mL, and minimal batch-to-batch variation (Figure 2D, 2E). The number of collected EVs were linearly proportional to the incubation time of the astrocytes, as they continuously proliferate in culture but presumably maintain their EV secretion rates. Although there was no significant difference in the number of collected EVs between 48 and 84 hours of astrocyte culture, we maintained all subsequent cultures to 84 hours to obtain the maximum number of EVs for use in downstream experiments before cells became overconfluent and started to deteriorate (Figure 2F, Figure S2). Long-term EV storage at temperatures below 4 °C and repeated freeze-thawing procedures did not cause significant change in their mode size, particle concentration, or total protein concentration (Figure 2G, 2H, 2I), indicating their stable nature in response to environmental changes. The mean zeta potential of the collected EVs was −10.37 mV, which indicated that the vesicles possessed a negative net surface charge (Figure 2J). The uniform surface charge prevented the aggregation of particles due to their electrical repulsion, leading to a stabilized nanoparticle suspension in the described system. Quantitative proteomics revealed that extracellular matrix proteins were the most abundant protein type inside the astrocyte-EVs, including fibronectin1 and collagen subtypes (Figure 2K).

3.3. Differentiated cortical neurons readily uptake astrocyte-derived EVs

For the next step, we investigated whether astrocyte-derived EVs can be internalized by human cortical neurons in culture. Antibodies against CD81 and the ExoGlow-protein EV labeling kit, which covalently label internal EV proteins, were used to cross-check EV-specific protein expression in the neuronal cytoplasm after EV treatment. The fluorescence signal from ExoGlow was optimized to monitor the neuronal uptake of EVs in a live cell culture environment. After 1 hour of EV treatment, followed by medium washing, 83.3% of neurons expressed fluorescence signal localized to their cell bodies, indicating successful uptake of astrocyte-derived EVs to the cytoplasm of cortical neurons (Figure 3A). However, due to the short duration of the activated fluorescence moiety, the fluorescence signal decayed rapidly after 2 hours of labeled EV treatment. To fluorescently quantify the amount of internalized EVs, we instead immunostained neurons with antibodies against CD81 (a common transmembrane protein on EV surface) after treating EVs with various cell to EV ratios. CD81 expression analysis revealed that EV-treated neurons exhibited significant increases in cytoplasmic fluorescence intensity in a dose-dependent manner, providing further evidence of successful internalization of EVs into the cultured neurons (Figure 3B). Fluorescence intensity dramatically increased when treating up to 25 EVs per cell and then reached a plateau, indicating that EV uptake saturated near the 25 EV particles per cell ratio (Figure 3C, 3D). Untreated neurons did not show CD81 positivity, not only indicating the

absence of EVs in the cell but also negligible levels of endogenous CD81 expression in the cultured neurons (Figure 3D).

3.4. Astrocyte-derived EV treatment inhibits neuronal apoptosis and senescence in cultured neurons

Since differentiation of cells in culture is an intrinsically stressful process, it is perhaps not surprising that the rapid (3 day) differentiation of neurons from hiPSCs in response to Ngn-2 overexpression produced high numbers of apoptotic cells. 92% of neurons without EV treatment expressed at least one of the apoptotic markers examined, whereas EV treated neurons contained a reduced population of early apoptotic cells. Increasing concentrations of EV treatments were found to correlate closely with the percentage of healthy living cells identified from each group, strongly implying a role for astrocyte-derived EVs in inhibiting neurons from entering the apoptotic pathway. Although the EVs did not effectively rescue cells already undergoing late stage apoptosis, an apparent trend towards a gradual reduction in the number of cells entering early stage apoptosis in all EV-treated groups suggests that bioactive molecules encapsulated in the EVs were able to rescue these cells from responding to pro-apoptotic signals in differentiating cultures (Figure 4A, 4B).

We also studied the effect of astrocyte-derived EVs on morphological degeneration in low density cultures to quantify any effect of the treatment on neuritic development. We plated early stage differentiated neurons (day 3) at 10,000 cells/cm^2, which constitutes 10% of our typical neuron plating density for long term culture. EVs were applied 1 hour after neuron plating and medium was replenished with fresh EV-supplemented medium every three days thereafter until the assay date. Untreated groups quickly began to show significant neuritic deterioration and cells did not survive beyond day 8 of culture. Conversely, EV-treated cultures showed normal axonal projections at day 4 and retained their robust morphology until day 8 (Figure S3A). Additionally, we tested whether low-density cortical neurons were susceptible to unusual cell senescence, and whether astrocyte-derived EVs could inhibit activation of senescent pathways in these cells. β-galactosidase (β-gal) is a hydrolase enzyme that catalyzes the hydrolysis of β-galactosides into monosaccharides in senescent cells that normally contain hyperactive lysosomes.[22,23] The cleavage of a chromogenic substrate (X-gal) solution by upregulated galactosidase activity results in the precipitation of a purple dye in the senescent cell cytoplasm. We used a β-gal solution kit on each group of neurons and analyzed the expression of X-gal cleavage-mediated dye precipitation in their cytoplasm. Low density neurons on day 4 without EV treatment clearly expressed dark blue aggregates in their cell bodies, strongly indicating that the cells had adopted a senescent state (Figure S3B). The number of β-gal positive neurons in the EV-treated group (1:100) were significantly less than that of untreated controls at day 4 of culture, indicating that the vesicular cargo was able to inhibit early neuronal senescence as well (Figure S3C).

3.5. EVs have limited effect on promoting neurite outgrowth and axon branching in hiPSC-derived cortical neurons

We investigated the effect of EV treatment on neuritic outgrowth in the early stages of culture and branching of axons at later stages. Neurons were treated with EVs on the day of plating and each of the cultures were imaged at different time points. The analysis of neuritic

outgrowth speed showed a marked increase in the longest neurite length between 6 hours and 12 hours post-plating for all conditions (Figure 5A, 5B). No significant difference in the early stage outgrowth speeds of neurites between EV untreated and EV-treated groups was observed, regardless of EV concentration examined (Figure 5B, 5C, 5D). Our data suggest that molecular cargos in the astrocyte-derived EVs do not play a role in regulating neurite development of human cortical neurons in culture.

3.6. Astrocyte-derived EV treatment enhances single cell electrophysiology of cortical neurons

Since astrocytes are actively involved in regulating electrochemical behavior of neurons in the CNS, we hypothesized that neuronal electrophysiology may be modulated by means of secreted astrocyte-derived EVs, based on the fact that the astrocytic coverage is limited to adjacent neurons, while consistent electrochemical regulation is required for neurons throughout the CNS. We therefore used whole cell patch-clamp techniques to investigate electrophysiological behavior in 4-week old cortical neuron cultures with or without astrocyte-derived EV treatment. Evoked action potential firing in neurons treated with EVs was significantly improved compared with untreated controls, in terms of repetitive firing behavior and action potential amplitude (Figure 6A). The population of neurons exhibiting repetitive firing behavior in response to 500 ms depolarizing current injections was much higher in the EV-treated group (50% of total) compared with that of untreated controls (30% of total) (Figure 6B). Due to the higher number of repetitive firing cells in astrocyte-derived EV treated cultures, treated neurons also exhibited a significant increase in average action potential firing frequency compared with untreated controls (Figure 6C). Similarly, we observed shorter action potential durations at 90% of repolarization (APD_{90}) in the EV treated neurons (5.61±0.08 ms) compared with untreated controls (6.89±0.33 ms) (Figure 6D). Together, these results indicate that the EV-treated neurons were more responsive to the input stimulus than neurons cultured without the aid of astrocyte-derived EVs. Specifically, the improvement in action potential firing frequency may indicate that the intracellular protein cascade (e.g. voltage-gated ion channels) that processes electrochemical stimuli in EV-assisted neurons was more highly developed than those of untreated control cells. In particular, the data suggest that activity of voltage-gated potassium channels might be affected by EV treatment since a significant improvement in action potential repolarization was observed in treated cells whereas the depolarization speed was consistent (Figure 6E, 6F). Finally, we compared resting membrane potential (RMP) between EV-treated and untreated neuronal populations. In these experiments, the average RMP of EV treated neurons was −61.6±2.0 mV, whereas untreated neurons exhibited an average RMP of −50±1.76 mV (Figure 6G). This significant decrease in RMP may indicate a greater capacity for transmembrane proteins in EV-treated cells to mediate passive K^+ membrane permeability, though further investigation of the mechanism is required. Another possible speculation is that the internalized EV cargos promoted the development of a more physiological K^+ gradient in the intracellular region of the cultured neurons. Such a result would therefore suggest that EV treated neurons promote the expression of more functional ion pumps and/or transporters.

3.7. Proteomics analysis identify EV cargo proteins that promote neuronal survival, oxidative stress management, and electrophysiological function

To identify molecular contributors to the above-mentioned physiological enhancement in EV treated cortical neurons, we performed a quantitative EV-proteomics assay. Mass spectrometry data processed with Proteome Discoverer produced a list of 875 proteins detected from three biological replicates of astrocyte conditioned medium. We then used gene ontology (GO) analysis to categorize the detected proteins in three major GO terms: cellular component, molecular function, and biological process. Nearly 60% of the detected proteins originated from extracellular exosomes while the rest were from cytoplasm, cytosol, and cell membrane. This result directly confirms that most of the proteins we analyzed were from an exosomal origin, since exosomes themselves are cytoplasm/cytosol derived (Figure 7A). This analysis further specifies that the EVs we collected are highly likely to be exosomes. A large portion of the listed proteins function for protein binding and cell-cell adhesion, likely indicating that many of the EV-associated proteins detected were involved in facilitating EV binding and uptake into the target cell, thus enabling its role as a potent intercellular transporter (Figure 7A-1, 7A-2). Using a list of common EV proteins reported by Choi *et al.* as a background, we then performed protein enrichment analysis by comparing astrocyte-derived EV protein levels to the background. Proteins identified from astrocyte-derived EVs were more heavily associated with integrin binding and extracellular matrix organization than common proteins found generally in EVs (Figure 7B). We then further characterized astrocyte-derived EVs specifically for their cohort of membrane proteins by referring to an up-to-date list of EV surface proteins reported by Wu *et al.*[24] CD81 was the most abundant membrane protein expressed on astrocyte-derived EVs, justifying our method of using CD81 as a reasonable marker for the identification and verification of neuronal EV uptake (Figure 7C). Although the majority of identified proteins work to support fundamental EV physiology and function, we sought to find neuroprotective proteins and proteins potentially involved in neuronal electrophysiology from the cargo protein profile. We found 40 proteins previously reported to negatively regulate cell apoptosis (10 of them were neuron-specific) such as HSP90AB1, α-synuclein, LRP1, and APOE (Figure 7D). Additionally, we found several cargo proteins that could potentially affect hiPSC-derived neuron electrophysiological function. These include Potassium channel tetramerization domain containing 12 (KCTD12), Glucose-6- phosphate dehydrogenase (G6PD), Kinesin family member 5B (KIF5B), Spectrin-alpha non-erythrocytic1 (SPTAN1) (Figure 7E).

4. Discussion

One possible mechanism of remote interaction between astrocytes and neurons is EV-mediated signaling. EVs such as exosomes are generated as intraluminal vesicles through inward budding of the multivesicular body; a subtype of late-stage endosomes.[25–32] Endogenously programmed intracellular trafficking of multivesicular bodies can either fuse them with lysosomes for subsequent degradation, or with the plasma membrane to facilitate the release of their vesicular contents into the extracellular space in the form of EVs.[25,31,32] In addition to the cellular ‘waste disposal’ role of EVs, they are now regarded as major carriers of soluble factors that mediate paracrine communication between various types of

cells within the CNS.[25,28] EVs encapsulate numerous proteins and transferrable mRNA, miRNA, lncRNA and lipids in order to modulate recipient cell behavior through post-transcriptional gene regulation, direct protein expression, or expression of transferred inhibitory RNAs[32]. For a detailed description of these vesicles, please see recent reviews (Zhang *et al.* 2019, Basso *et al.* 2016).

The role of astrocyte-derived EVs in different neuronal subtypes has been studied in several *in vitro* and animal model studies. These previous studies focused on phenotypic changes that occur in EV secreting cells in response to various extracellular stimuli, such as inflammatory cytokine treatment, which can result in significant changes to their EV profile and in turn induce remarkable degeneration in neurons taking up these EVs.[11,13,16,17,33] Despite these studies significantly expanded our understanding of how astrocyte-derived EVs regulate their function to modulate neuronal physiology, phenotypic disparity of astrocytes in the CNS of human and murine models has meant that a reliable understanding of human astrocyte EV-based neuroglial communication remains elusive. Moreover, previously published studies have primarily investigated the effect of astrocyte-derived EVs on neuronal survival, morphological development, and population level electrophysiology using murine-derived cells and multi-electrode array systems.[13] While informative as a means to widen our basic understanding of EV-mediated neuroglial communication, such studies are insufficient to delineate astrocyte-EV's comprehensive effect on the electrophysiological function of single neurons, and more importantly, to define the EV cargo molecules that drive the reported physiological effects in treated cells. In this study, we sought to elucidate the effect of astrocyte-derived EVs on hiPSC-derived neurons, focusing on their role in enhancing electrochemical function. Moreover, we analyzed the cargo protein profile using EV-proteomics to identify those proteins likely responsible for the physiological enhancements we observed.

We first confirmed the identity of hiPSC neurons differentiated for this study. The Ngn2 overexpressing i^{3}N iPSCs developed by Wang *et al.* were used for rapid differentiation into highly homogeneous human cortical neurons.[18] Doxycycline-induced differentiation generated CUX-1 and MAP-2 positive cortical neurons after just 3 days in culture and these neurons were found to be capable of absorbing EVs from the culture medium, likely via standard EV uptake mechanisms described elsewhere.[27,34] Although the majority of the population in culture exhibited a cortical neuron identity, as determined by expression of the above mentioned markers, the survival and function of these cells following Ngn2 overexpression was not yet determined. Therefore, we measured their baseline health and function using apoptotic markers, a senescence marker, and single cell electrophysiological analysis in the absence of glial-derived support. Flow cytometry results using two different apoptosis markers (Annexin V and propidium iodide) illustrated that the majority of these neurons at 3 days post-induction were already apoptotic. Though the signaling mechanisms controlling neuronal apoptosis in adult nerve tissue are not fully understood, previous studies have suggested a lack of paracrine trophic factors such as neurotrophins and IGF-1 may lead to apoptotic cell death.[35,36] Other previous observations have led to the hypothesis that deregulation of the cell cycle can directly trigger apoptosis or oxidative stress can affect cell cycle machinery to promote apoptosis.[37,38] Insufficient provision of growth factors and/or tolerance of oxidative stress are potent factors in driving the onset of

neurodegenerative disease. As such, the lack of direct support from glial cells in purified cultured neurons may lead to misinterpretation of assay results, especially in neurodegenerative disease modeling studies. Given that neuronal apoptosis is not a cell-autonomous behavior, we treated astrocyte-derived EVs to early stage (day 3) cultured neurons to check whether the vesicular cargos could enhance neuron survival in culture. We confirmed that neuronal apoptosis was evidently ameliorated following EV treatment and that survival improved in dose dependent manner. Our results may imply that astrocyte-derived EV cargoes function to prevent initiation or early progression of neuronal apoptosis, but cannot reverse late stage progression in cells that are already committed to apoptotic cell death. Our results correlate with a previous study using a rodent model that showed expression of various neuroglobins in astrocytes exhibited an anti-apoptotic effect and suggested that such factors might function as neuroprotective against endogenous and environmental stressors.[39,40] We then tried to define the cargo proteins responsible for this improvement by running EV-proteomics analysis. Gene ontology analysis of the identified astrocyte-EV proteins identified 40 proteins that were previously reported to negatively regulate the cell apoptosis signal. 10 of these proteins were neuron-specific, including heat shock protein HSP90AB1, alpha-synuclein (SNCA), and low-density lipoprotein receptor-related protein 1 (LRP1). Heat shock protein 90AB1, which functions as a molecular chaperone to counteract cellular stress, was the most abundant among the anti-apoptotic regulator proteins present in the EVs. Carnemolla *et al.* showed that astrocytes and oligodendrocytes transcribe the HSP90aa1 and HSP90ab1 genes especially under heat shock response inhibited proteotoxic condition. Additionally, Batulan *et al.* reported the inability of differentiated neurons to transcriptionally induce endogenous heat shock responses after external stress in rodent model experiments.[41] These results, coupled with those presented here, suggest that astroglial heat shock protein support (rather than endogenous HSP expression in neurons) helps alleviate stress in neurons and that this interaction is mediated via EVs.

Additionally, EV treatment on low density neurons induced notable decreases in senescence marker expression. Proteomic analysis revealed calreticulin (CRT) expression in the EV cargoes (Table S1). CRT is a highly conserved chaperone protein that predominantly resides in the endoplasmic reticulum. CRT has been reported to block the translation of p21 via stabilization of the 5’ region of its mRNA, leading to the repression of p21 protein expression.[42] P21 is known to drive cell growth arrest and senescence, therefore its suppression should also repress senescent behavior. Taken together, our data highlight a neuromodulatory function for astrocyte-EV cargo proteins that inhibits neuronal apoptosis and senescence triggered by stressful conditions in culture.

We next evaluated neuritic outgrowth speed and neurite length in EV treated neurons. A recent study using 3D co-cultures of neurons and astrocytes showed an interdependent structural development in these cell populations.[43] Astrocyte addition promoted denser dendrite development and longer axons in neurons while astrocytes also benefitted in terms of enhanced cytoskeletal outgrowth and proliferation. The study additionally illustrated that the degree to which astrocytic aid contributed to neuronal axon and dendrite development was highly dependent on the distance between the two cell types in culture. Astrocyte’s structural support was significantly reduced in distal neurons, indicating their close contact

is required for astrocyte-aided neurite development in neurons.[43] Similar to this result, we did not see meaningful enhancement of neuritic outgrowth speed nor axon length in EV treated neurons, reconfirming that astrocyte's structural support on developing neurons is unlikely to be provided via remote, EV-mediated interaction.

Since the major physiological function of neurons in the cerebral cortex is their inter-neuronal electrochemical signal transmission, considerable effort has been made to elucidate the role of astrocytes in promoting synaptogenesis and synapse maturation. Rodent model studies found that neurogenesis precedes astrogenesis in the cortex, but neuronal synapses do not form until the end of astrogenesis.[44] They also form 'tripartite' synapses with pre-synapsed neurons, increasing synaptic diversity and buffering neurotransmitter concentrations within the synaptic cleft to maintain electrochemical homeostasis. Although their critical role in intercellular synapse development is well defined in rodents, it has yet to be defined how astrocytes modulate the functional maturation of developing neurons, particularly in the human cortex. Here, we hypothesized that secreted factors from astrocytes contribute to the maturation of electrophysiological function in human cortical neurons, and demonstrated that astroglial-derived EVs significantly enhance single neuron electrophysiology as determined by whole-cell patch clamp experiment.

Whole cell patch-clamp recording enables comprehensive electrophysiological assessment of individual neurons, by measuring resting membrane potential, input resistance and capacitance, and waveform analysis for evoked or spontaneous action potentials.[45] The characteristics of action potentials, such as depolarization and repolarization speed, action potential amplitude and frequency, action potential duration, along with the amplitude of sodium and potassium currents, are all important criteria for the validation of the functional maturity of neurons. Maximum frequency of action potential firing indicates how well neurons can repeat the action potential firing cycle in response to protracted depolarizing stimuli and depends on the strength of stimulus applied to the neurons. The nervous system in our body is frequency-modulated, rather than amplitude modulated, meaning that the intensity of a stimulus does not affect the action potential amplitude but it's frequency. With these metrics, we examined whether astrocyte-EVs act to enhance any aspects of electrophysiological maturation in cultured cortical neurons. We observed extensive improvement in the majority of examined electrophysiological metrics in EV treated neurons. EV-treated neurons exhibited more repetitive and consistent firing of action potentials in response to protracted depolarizing stimuli as well as significantly lower resting membrane potentials than untreated neurons. Previous studies have shown that addition of rat astrocytes to hiPSC-neural cultures induces dramatic enhancement of functional development in neurons, in terms of dendritic arborization, electrochemical excitability, and synapse formation. However, the underlying intercellular mechanism facilitating this positive regulation was not elucidated. Based on our results, we can postulate that ion channel expression in early stage hiPSC neurons may depend on the support of astroglial proteins and/or RNAs provided through remote molecular transmission.

To investigate the molecular drivers of the electrophysiological improvement observed in this study, we analyzed the cargo proteins collected within astrocyte-derived EVs. Proteomic analysis found the presence of proteins promoting excitability of neurons, such as KCTD12,

KIF5B, G6PD, and SPTAN1. Potassium channel tetramerization domain containing 12 (KCTD), an important protein for neuronal excitability control, is known to increase $GABA_B$ receptor expression in neurons, which acts in an excitatory manner during early stages of neuron development in contrast to their inhibitory role in the mature CNS.[46,47] Kinesin family member 5B (KIF5B) is a subtype of homologous kinesin 1 proteins with the primary role of mediating long-distance molecular transport in neurons. Most of the previous studies focused on their role as molecular motors, but a recent study showed KIF5B has distinct functions in excitatory synapse and ion channel development and function. Knock-out of KIFB (but not other KIF5s) induced significant reduction in the frequency of excitatory current generation in rodent models.[48] Additionally, Su *et al.* reported the KIF5B regulates the axonal transport of voltage-gated sodium channels, thereby indirectly controlling the excitatory electrochemical activity of neurons in the CNS.[49]

Increased activity of Glucose-6- phosphate dehydrogenase (G6PD) is known to protect neurons from Parkinsonism, mainly by protecting them from oxidative damage. Experiments conducted by Loniewska *et al.* demonstrated that G6PD deficient mice exhibit significant cognitive abnormalities and fail to replenish antioxidant glutathione, which detoxifies neurodegenerative reactive oxygen species (ROS) in neurons.[50] Neurons are one of the most vulnerable cell types to oxidative stress and reactive oxygen metabolites are known to act to modify ion transport mechanisms via ion transport pathway proteins.[51] As such, stable ROS handling ability in neurons may constitute a critical prerequisite to facilitate normal ion channel activities associated with electrophysiological function. Previous studies have revealed that ROS can attack ion channel transporters directly or indirectly through lipid peroxidation.[52] The disruption caused by accumulation of ROS stress on neuron membranes has been reported to alter membrane potential and current, ionic gradient, action potential duration and amplitude, spontaneous excitability, and even resting membrane potentials.[53] Hool *et al.* also demonstrated that ROS stress targets voltage-gated Na^+, K^+, Ca^{2+}, and Ca^{2+}-gated K^+ channels, and interferes with ATP-sensitive K^+ currents and L-type Ca^{2+} currents.[54,55] The fact that CNS neurons have a limited antioxidant capacity, and rely heavily on astroglial support to deal with oxidative stress, makes inclusion of G6PD in the astrocyte-derived EVs a reasonable mechanism to facilitate remote support for neuronal ROS handling. Interestingly, one of the most prominent ROS (hydrogen peroxide) is known to delay the inactivation of sodium currents through altering K^+ channel activity.[53] Since we observed a dramatic ability for EV treatment to improve repolarization of cortical neurons but exerted little modulating effect on the depolarization speed, we postulate that antioxidant support from astrocyte-EVs may contribute to the restoration of a neuron's repolarization function. Given that ROS mediated stress is known to be involved in the pathology of numerous neurodegenerative diseases, these results highlight the importance of further in-depth study into the molecular mechanisms that underlie ROS stress-induced ion channel disruption. Such future work could help define common pathologic mechanisms across multiple disease states and identify potential therapeutic targets with which to combat neurodegeneration in the human CNS.

We also found small quantities of alpha II-spectrin within astrocyte-EV cargoes, that potentially work to stabilize Na^+ channels. Galiano *et al.* reported the alpha II-spectrin stabilizes nascent sodium channel clusters in cortical neurons and regulates the assembly of

the node of Ranvier.[56] Mutations in alpha II-spectrin are a known cause of early infantile epileptic encephalopathies, and have been shown to alter the sensitivity of voltage-gated sodium channels, leading to abnormal action potential thresholds in infant nerves.[57] Additionally, the presence of EHD3 proteins in astrocyte-EVs, which has been shown to regulate membrane excitability in neurons, could help explain the observed improvement in action potential firing behavior in EV-treated neurons.[58] EHD3 in known to be differentially expressed in pyramidal neurons of the pre-frontal cortex in patients with schizophrenia, further underscoring its physiological role in modulating electrochemical behavior in cortical neurons.[59]

5. Conclusion

In this study, we have investigated the extensive physiological effects of EVs secreted from human astrocytes on hiPSC-derived cortical neurons. Treatment with an optimized EV concentration was found to have a significant impact on the inhibition of neuronal apoptosis, presumably due to the presence of anti-apoptotic proteins within the EVs. Additionally, we showed that EV treatment prevents early senescence and improves the longevity of cortical neurons in culture. EVs also remarkably altered the electrophysiology of single neurons. We observed a 40% increase in the number of neurons exhibiting repetitive action potential firing behavior, three times higher maximum frequency in action potential firing, and an 18.5% reduction in the APD_{90} of EV-treated neurons compared with untreated controls. EV-treated neurons also showed a significant reduction in resting membrane potential and faster repolarization speed, which all indicate a positive effect of astrocyte-derived EVs on their functional maturation. We also characterized the protein profile of astrocyte-derived EVs to identify protein cargos responsible for this dramatic enhancement of electrophysiological function. Several astrocyte proteins known to be involved in regulating neuronal ion channel maturation, membrane excitability, and oxidative stress handling were detected, which could explain the functional enhancement of cultured neurons post EV treatment. The observations presented here provide useful insights on the diverse modes of neuron-glia communication in the human CNS. These data may inform on the use of EVs for developing more physiologically relevant nerve-on-a-chip assays for preclinical screening applications, enhancing our capacity to model various types of neuropathies, and even the development of novel therapies or biomarkers critical for combating neurodegenerative diseases in the future.

Supplementary Material

Refer to Web version on PubMed Central for supplementary material.

Acknowledgements

This work was supported by the Korea Health Technology R&D Project through the Korea Health Industry Development Institute (KHIDI), funded by the Ministry of Health & Welfare, Republic of Korea (HI19C0642 to D.H.K), the National Institute of Neurological Disorders and Stroke (R01 NS094388 to D.H.K), Bio & Medical Technology Development Program of the National Research Foundation of Korea (NRF) funded by the Ministry of Science and ICT (MSIT) (2016M3A9C6917402 to J.B.L), as well as NIH KL2 TR002317 (to A.S.T.S). We thank Dr. Bruce Conklin for providing iPSCs harboring an inducible Ngn 2 transgene, Dr. Kim Woodrow for using Nanoparticle Tracking Analyzer use and Dr. Stuart Shankland for using ultracentrifuge equipment for isolating the EVs.

Data Availability

The raw data required to reproduce these findings are available to download from https://data.mendeley.com/datasets/2kw7tgph94/1. The processed data required to reproduce these findings are available to download from https://data.mendeley.com/datasets/2kw7tgph94/1.

References

1. Farhy-Tselnicker I & Allen NJ Astrocytes, neurons, synapses: A tripartite view on cortical circuit development. Neural Dev 13, 1–12 (2018). [PubMed: 29325591]
2. Molnár Z et al. New insights into the development of the human cerebral cortex. J. Anat 432–451 (2019). 10.1111/joa.13055 [PubMed: 31373394]
3. Rakic P & Lombroso PJ Development of the cerebral cortex: I. Forming the cortical structure. J. Am. Acad. Child Adolesc. Psychiatry 37, 116–117 (1998). [PubMed: 9444908]
4. Harris KD & Mrsic-Flogel TD Cortical connectivity and sensory coding. Nature 503, 51–58 (2013). [PubMed: 24201278]
5. Douglas RJ & Martin KAC Neuronal Circuits of the Neocortex. Annu. Rev. Neurosci 27, 419–451 (2004). [PubMed: 15217339]
6. Dzyubenko E, Gottschling C & Faissner A Neuron-Glia Interactions in Neural Plasticity: Contributions of Neural Extracellular Matrix and Perineuronal Nets. Neural Plast 2016, 5214961 (2016). [PubMed: 26881114]
7. Shi Y, Kirwan P & Livesey FJ Directed differentiation of human pluripotent stem cells to cerebral cortex neurons and neural networks. Nat. Protoc 7, 1836–1846 (2012). [PubMed: 22976355]
8. Luarte A et al. Astrocytes at the Hub of the Stress Response: Potential Modulation of Neurogenesis by miRNAs in Astrocyte-Derived Exosomes. Stem Cells Int 2017, (2017).
9. Bellot-Saez A, Kékesi O, Morley JW & Buskila Y Astrocytic modulation of neuronal excitability through K+spatial buffering. Neurosci. Biobehav. Rev 77, 87–97 (2017). [PubMed: 28279812]
10. Hansen MG, Tornero D, Canals I, Ahlenius H & Kokaia Z In vitro functional characterization of human neurons and astrocytes using calcium imaging and electrophysiology. Methods Mol. Biol 1919, 73–88 (2019). [PubMed: 30656622]
11. Ibáñez F, Montesinos J, Ureña-Peralta JR, Guerri C & Pascual M TLR4 participates in the transmission of ethanol-induced neuroinflammation via astrocyte-derived extracellular vesicles. J. Neuroinflammation 16, 1–14 (2019). [PubMed: 30606213]
12. Hira K et al. Astrocyte-derived exosomes treated with a semaphorin 3A inhibitor enhance stroke recovery via prostaglandin D2 synthase. Stroke 49, 2483–2494 (2018). [PubMed: 30355116]
13. You Y et al. Activated human astrocyte-derived extracellular vesicles modulate neuronal uptake, differentiation and firing. J. Extracell. Vesicles 9, (2020).
14. Pascua-Maestro R et al. Extracellular vesicles secreted by astroglial cells transport apolipoprotein D to neurons and mediate neuronal survival upon oxidative stress. Front. Cell. Neurosci 12, 1–13 (2019).
15. Datta Chaudhuri A et al. Stimulus-dependent modifications in astrocyte-derived extracellular vesicle cargo regulate neuronal excitability. Glia 68, 128–144 (2020). [PubMed: 31469478]
16. Varcianna A et al. Micro-RNAs secreted through astrocyte-derived extracellular vesicles cause neuronal network degeneration in C9orf72 ALS. EBioMedicine 40, 626–635 (2019). [PubMed: 30711519]
17. Silverman JM et al. CNS-derived extracellular vesicles from superoxide dismutase 1 (SOD1)G93A ALS mice originate from astrocytes and neurons and carry misfolded SOD1. J. Biol. Chem 294, 3744–3759 (2019). [PubMed: 30635404]
18. Wang C et al. Scalable Production of iPSC-Derived Human Neurons to Identify Tau-Lowering Compounds by High-Content Screening. Stem Cell Reports 9, 1221–1233 (2017). [PubMed: 28966121]
19. Fernandopulle MS et al. Transcription Factor-Mediated Differentiation of Human iPSCs into Neurons. Curr. Protoc. Cell Biol 79, e51 (2018). [PubMed: 29924488]

20. Gunhanlar N et al. A simplified protocol for differentiation of electrophysiologically mature neuronal networks from human induced pluripotent stem cells. Mol. Psychiatry 23, 1336–1344 (2018). [PubMed: 28416807]
21. Patani R et al. Retinoid-independent motor neurogenesis from human embryonic stem cells reveals a medial columnar ground state. Nat. Commun 2, (2011).
22. de Mera-Rodríguez JA et al. Senescence-associated β-galactosidase activity in the developing avian retina. Dev. Dyn 248, 850–865 (2019). [PubMed: 31226225]
23. Tominaga T, Shimada R, Okada Y, Kawamata T & Kibayashi K Senescence-associated-β-galactosidase staining following traumatic brain injury in the mouse cerebrum. PLoS One 14, 1–17 (2019).
24. Wu D et al. Profiling surface proteins on individual exosomes using a proximity barcoding assay. Nat. Commun 10, 1–10 (2019). [PubMed: 30602773]
25. Basso M & Bonetto V Extracellular vesicles and a novel form of communication in the brain. Front. Neurosci 10, 1–13 (2016). [PubMed: 26858586]
26. Gangoda L, Boukouris S, Liem M, Kalra H & Mathivanan S Extracellular vesicles including exosomes are mediators of signal transduction: Are they protective or pathogenic? Proteomics 15, 260–271 (2015). [PubMed: 25307053]
27. Mulcahy LA, Pink RC, Raul D & Carter F Routes and mechanisms of extracellular vesicle uptake 1, 1–14 (2014).
28. Paolicelli RC, Bergamini G & Rajendran L Cell-to-cell Communication by Extracellular Vesicles: Focus on Microglia. Neuroscience 405, 148–157 (2019). [PubMed: 29660443]
29. Saeedi S, Israel S, Nagy C & Turecki G The emerging role of exosomes in mental disorders. Transl. Psychiatry 9, 122 (2019). [PubMed: 30923321]
30. Lee Y, El Andaloussi S & Wood MJA Exosomes and microvesicles: Extracellular vesicles for genetic information transfer and gene therapy. Hum. Mol. Genet 21, 125–134 (2012).
31. Frühbeis C, Fröhlich D & Krämer-Albers EM Emerging roles of exosomes in neuron-glia communication. Front. Physiol 3 4, 1–7 (2012). [PubMed: 22275902]
32. Hessvik NP & Llorente A Current knowledge on exosome biogenesis and release. Cell. Mol. Life Sci 75, 193–208 (2018). [PubMed: 28733901]
33. Keir ME, Butte MJ, Freeman GJ & Sharpe AH PD-1 and Its Ligands in Tolerance and Immunity. Annu. Rev. Immunol 26, 677–704 (2008). [PubMed: 18173375]
34. Holm MM, Kaiser J & Schwab ME Extracellular Vesicles: Multimodal Envoys in Neural Maintenance and Repair. Trends Neurosci 41, 360–372 (2018). [PubMed: 29605090]
35. Johnson F, Hohmann SE, DiStefano PS & Bottjer SW Neurotrophins suppress apoptosis induced by deafferentation of an avian motor-cortical region. J. Neurosci 17, 2101–2111 (1997). [PubMed: 9045737]
36. Lindholm D, Carroll P, Tzimagiorgis G & Thoenen H Autocrine-paracrine regulation of hippocampal neuron survival by IGF-1 and the neurotrophins BDNF, NT-3 and NT-4. Eur. J. Neurosci 8, 1452–1460 (1996). [PubMed: 8758952]
37. Redza-Dutordoir M & Averill-Bates DA Activation of apoptosis signalling pathways by reactive oxygen species. Biochim. Biophys. Acta - Mol. Cell Res 1863, 2977–2992 (2016).
38. Elmore S Apoptosis: A Review of Programmed Cell Death. Toxicol. Pathol 35, 495–516 (2007). [PubMed: 17562483]
39. Guidolin D, Tortorella C, Marcoli M, Maura G & Agnati LF Neuroglobin, a Factor Playing for Nerve Cell Survival. Int. J. Mol. Sci 17, 1–16 (2016).
40. Baez E et al. Protection by neuroglobin expression in brain pathologies. Front. Neurol 7, 1–10 (2016). [PubMed: 26834696]
41. Batulan Z et al. High threshold for induction of the stress response in motor neurons is associated with failure to activate HSF1. J. Neurosci 23, 5789–5798 (2003). [PubMed: 12843283]
42. Iakova P et al. Competition of CUGBP1 and calreticulin for the regulation of p21 translation determines cell fate. EMBO J 23, 406–417 (2004). [PubMed: 14726956]
43. Fang A et al. Effects of astrocyte on neuronal outgrowth in a layered 3D structure. Biomed. Eng. Online 18, 1–16 (2019). [PubMed: 30602383]

44. Farhy-Tselnicker I & Allen NJ Astrocytes, neurons, synapses: A tripartite view on cortical circuit development. Neural Dev 13, 1–12 (2018). [PubMed: 29325591]
45. Petersen CCH Whole-Cell Recording of Neuronal Membrane Potential during Behavior. Neuron 95, 1266–1281 (2017). [PubMed: 28910617]
46. Li M et al. KCTD12 modulation of GABA(B) receptor function. Pharmacol. Res. Perspect 5, 1–9 (2017).
47. Teng X et al. KCTD: A new gene family involved in neurodevelopmental and neuropsychiatric disorders. CNS Neurosci. Ther 25, 887–902 (2019). [PubMed: 31197948]
48. Zhao J et al. Specific depletion of the motor protein KIF5B leads to deficits in dendritic transport, synaptic plasticity and memory. Elife 9, 1–34 (2020).
49. Su YY et al. KIF5B promotes the forward transport and axonal function of the voltage-gated sodium channel Nav1.8. J. Neurosci 33, 17884–17896 (2013). [PubMed: 24198377]
50. Loniewska MM et al. DNA damage and synaptic and behavioural disorders in glucose-6-phosphate dehydrogenase-deficient mice. Redox Biol 28, 101332 (2020). [PubMed: 31581069]
51. Wang X & Michaelis EK Selective neuronal vulnerability to oxidative stress in the brain. Front. Aging Neurosci 2, 1–13 (2010). [PubMed: 20552041]
52. Kiselyov K & Muallem S ROS and intracellular ion channels HHS Public Access. Cell Calcium 60, 108–114 (2016). [PubMed: 26995054]
53. Jovanovi Z Effects of Oxidative Stress on the Electrophysiological Function of Neuronal Membranes. Oxidative Stress Dis (2012). 10.5772/33580
54. Hermann A, Sitdikova GF & Weiger TM Oxidative stress and maxi calcium-activated potassium (BK) channels. Biomolecules 5, 1870–1911 (2015). [PubMed: 26287261]
55. Sahoo N, Hoshi T & Heinemann SH Oxidative modulation of voltage-gated potassium channels. Antioxidants Redox Signal 21, 933–952 (2014).
56. Galiano MR et al. Controls Axon Initial Segment Assembly. Cell 149, 1125–1139 (2013).
57. Tohyama J et al. SPTAN1 encephalopathy: Distinct phenotypes and genotypes. J. Hum. Genet 60, 167–173 (2015). [PubMed: 25631096]
58. EHD3-Dependent Endosome Pathway Regulates Cardiac Membrane Excitability and Physiology. Circ Res 23, 1–7 (2008).
59. Prabakaran S et al. Mitochondrial dysfunction in schizophrenia: Evidence for compromised brain metabolism and oxidative stress. Mol. Psychiatry 9, 684–697 (2004). [PubMed: 15098003]
60. Choi DS, Kim DK, Kim YK & Gho YS Proteomics, transcriptomics and lipidomics of exosomes and ectosomes. Proteomics 13, 1554–1571 (2013). [PubMed: 23401200]

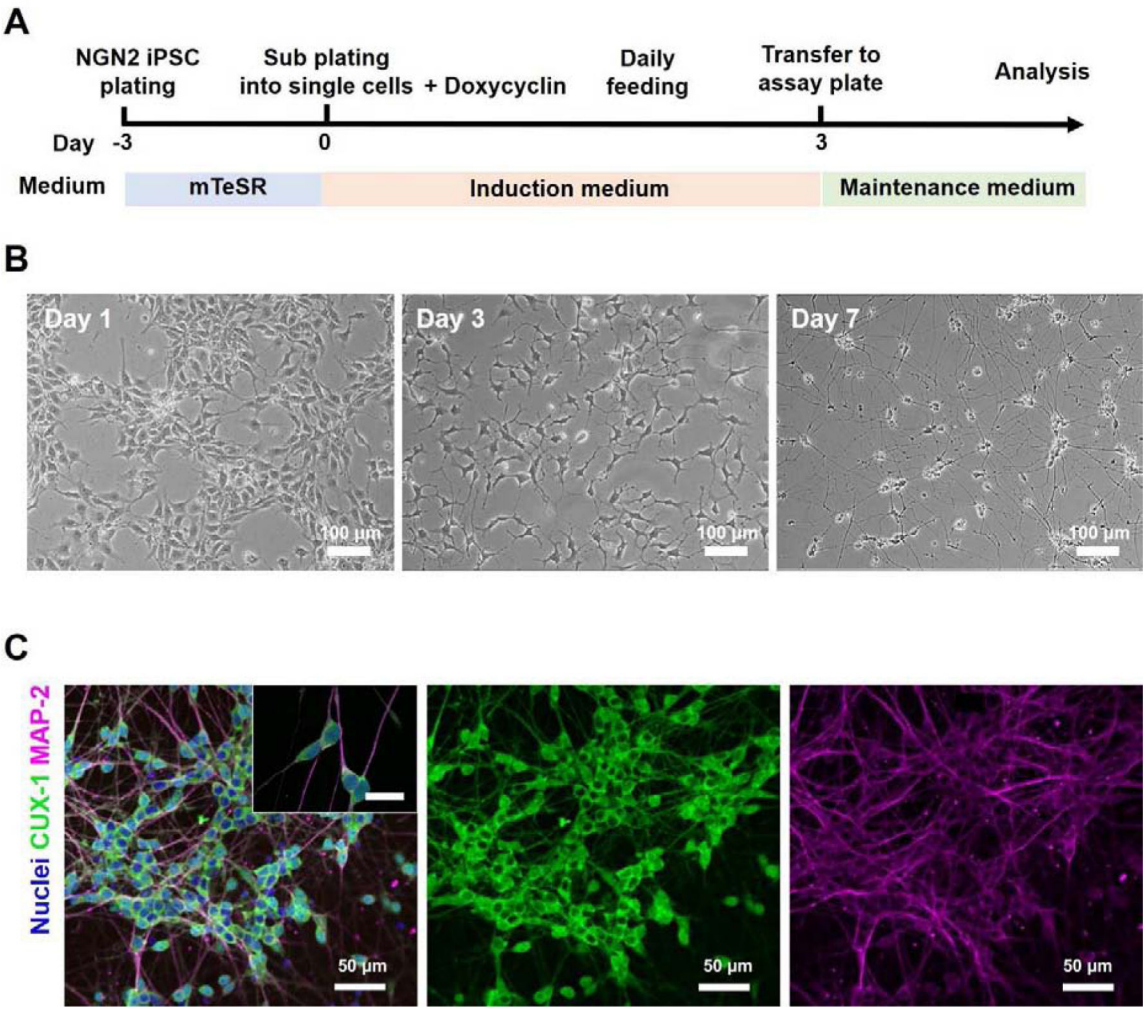

Figure 1. Differentiation of cortical neurons from Ngn 2 overexpressing hiPSCs.

(A) Differentiation protocol highlighting the use of doxycyclin to initiate Ngn 2 transcription. (B) Morphological changes observed between initial stages of differentiation and the later stages of culture. (C) Human iPSC-derived cortical neurons immunostained using antibodies against CUX-1 (neuronal marker in cerebral cortex layers 2 and 3) and MAP2 (pan-neuronal marker) with DAPI-stained nuclei. Inset shows clear expression of CUX-1 in the cell cytoplasm. Scale bar of inset image: 20 µm.

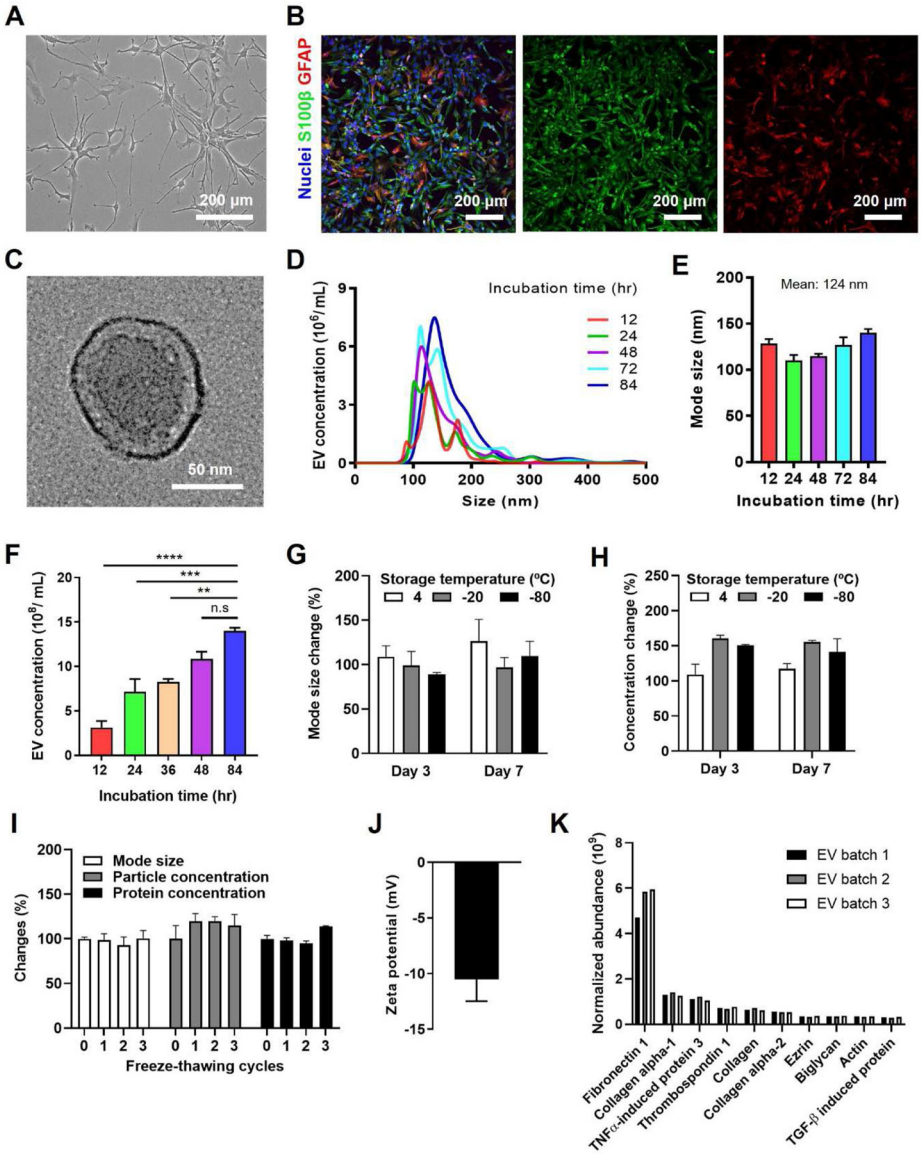

Figure 2. Astrocyte identification and EV characterization

(A) Bright field image of human primary astrocytes at day 3 of culture. (B) Astrocyte culture immunostained using antibodies against GFAP and S100β; glial cell markers primarily expressed in astrocytes. (C) TEM images of EVs collected from primary astrocytes. (D) Size distribution of collected EVs with various cell incubation time before EV collection. (E) Mode size of collected EVs with various incubation time measured by NTA (Nanoparticle Tracking Analysis). Incubation times on the x axis indicate the time elapsed following EV-free medium change at day 4. (F) Number of particles per mL in the EV solution with the various astrocyte incubation times. Effect of long-term storage at different temperatures on EV mode size change (G) and particle concentration change (H). (I) Effect of repeated freeze-thaw cycles on EV mode size, particle concentration, and total protein concentration. (J) Zeta-potential of collected EVs after 84 hours of cell incubation. (K) The ten most

abundant proteins detected in the EVs. In all presented data, error bars are SD and **p< 0.005 ***p<0.0005 ****p<0.0001, ns not significant (n=3).

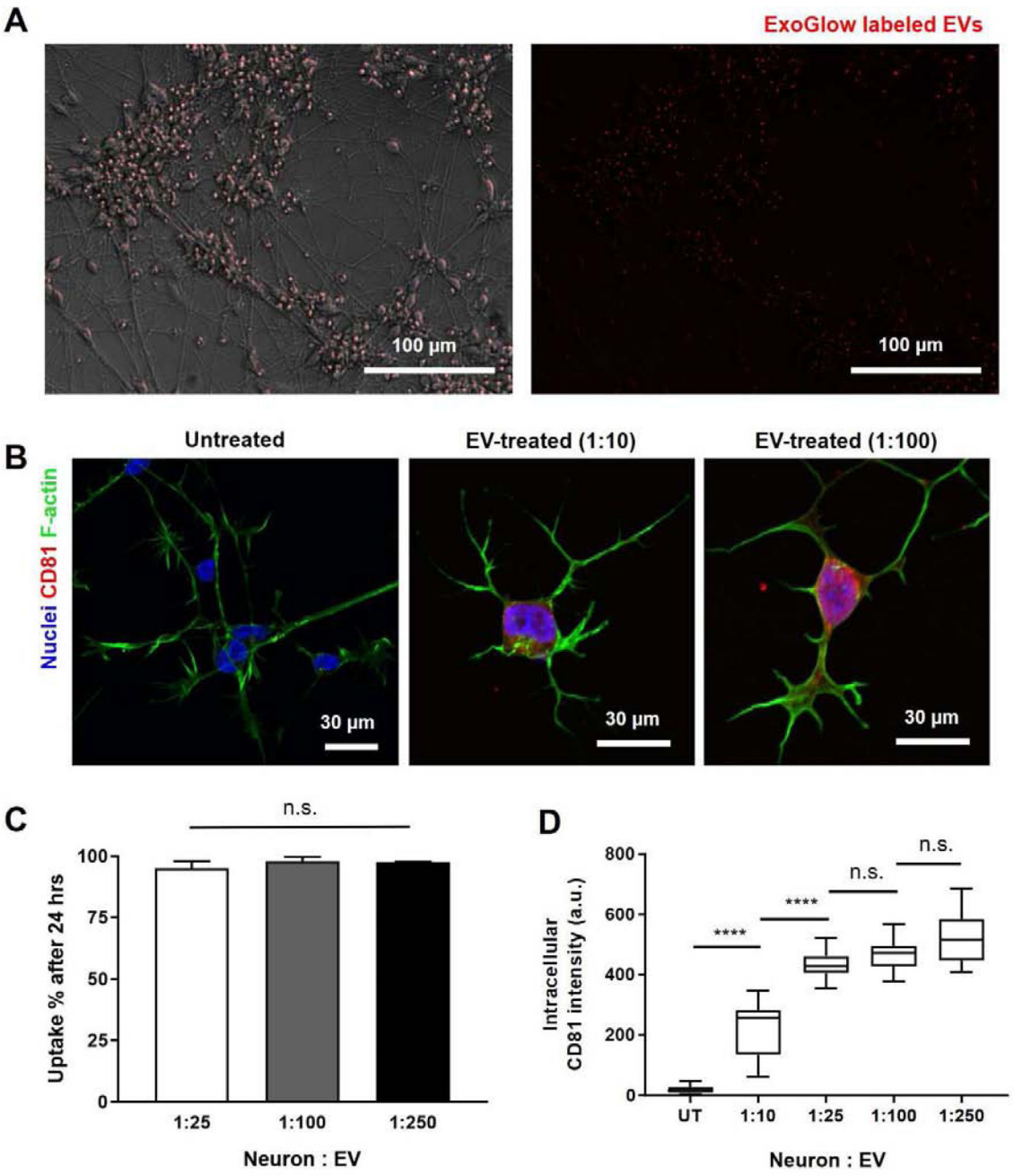

Figure 3. EV internalization assay using EV-specific markers

(A) Live cell images of cortical neurons illustrating localization of EVs stained with the ExoGlow EV-protein staining kit for 1 hour. (B) Representative cortical neurons double immunostained with antibodies against CD81 and F-actin to demonstrate cytoplasmic internalization of differing amounts of EVs. (C) The uptake efficiency of EVs at different neuron to EV ratios obtained by quantifying fluorescently labeled EVs. (D) The relationship between CD81 fluorescent intensity in EV-treated cells with different cell to EV ratio. The fluorescence intensity is expressed as relative values normalized to an untreated sample. In all presented data, **p<0.005 ***p<0.0005 ****p<0.0001, ns not significant (n = 3).

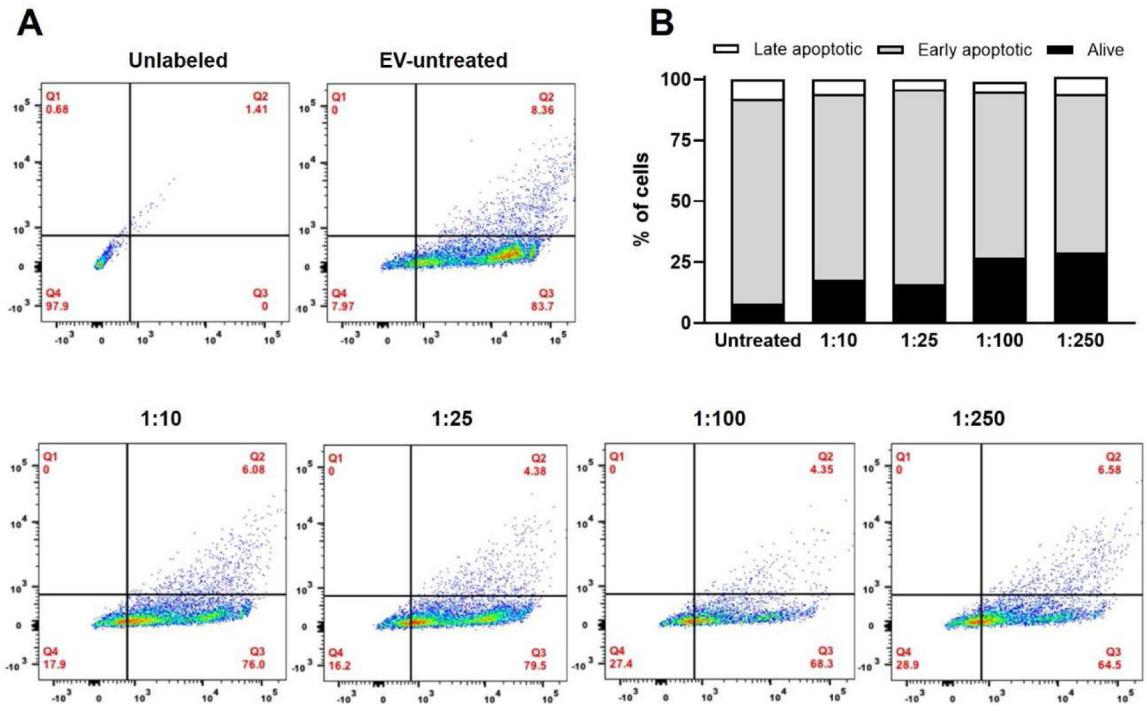

Figure 4. Analysis of apoptotic neurons in response to treatment with various concentrations of astrocyte-derived EVs

(A) Flow cytometry analysis of neurons at day 6 using Annexin V (y axis) and propidium iodide (x axis). The inset numbers indicate the percentage of cells occupying each quadrant. Q1 = early-stage apoptotic cells (PI positive), Q2 = late-stage apoptotic cells (both PI and Annexin V positive), Q3 = early-stage apoptotic cells (Annexin V positive), Q4 = alive cells (PI and Annexin V negative). 10,000 cells per condition were used for this assay. (B) Quantification and comparison of the number of analyzed cells correspond to each condition. A contingency table comparing EV treatment conditions against apoptosis found that the two factors are significantly related ($p = 0.008$, Chi squared test), suggesting that the occurrence of neuronal apoptosis is dependent on the amount EVs added in the culture medium.

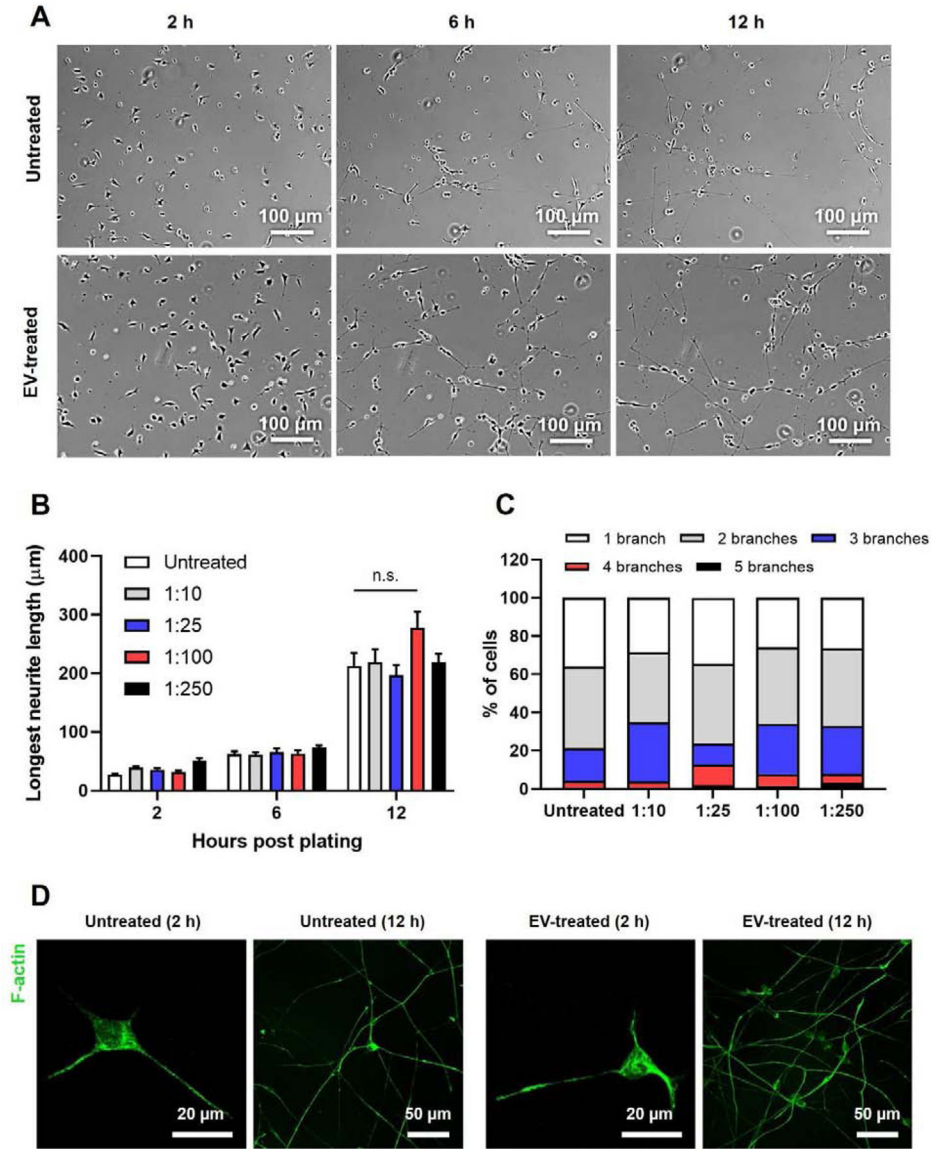

Figure 5. Neurite outgrowth speed and axon branching analysis from EV treated and untreated neurons.

(A) Morphological comparison of neurons plated in low density with and without EV treatment at three different time points. (B) Quantitative analysis of the longest neurite length in each culture condition. Error bars represent standard error of the mean (n = 19). (C) The population of neurons exhibiting different numbers of axon branches in each culture condition (n = 19). A contingency table comparing EV treatment conditions against number of branches in neurons found that the two factors are not significantly related (p = 0.06, Chi squared test). (D) Representative immunostained images of neurons stained for neurofilament expression to label axons at different timepoints from each culture condition.

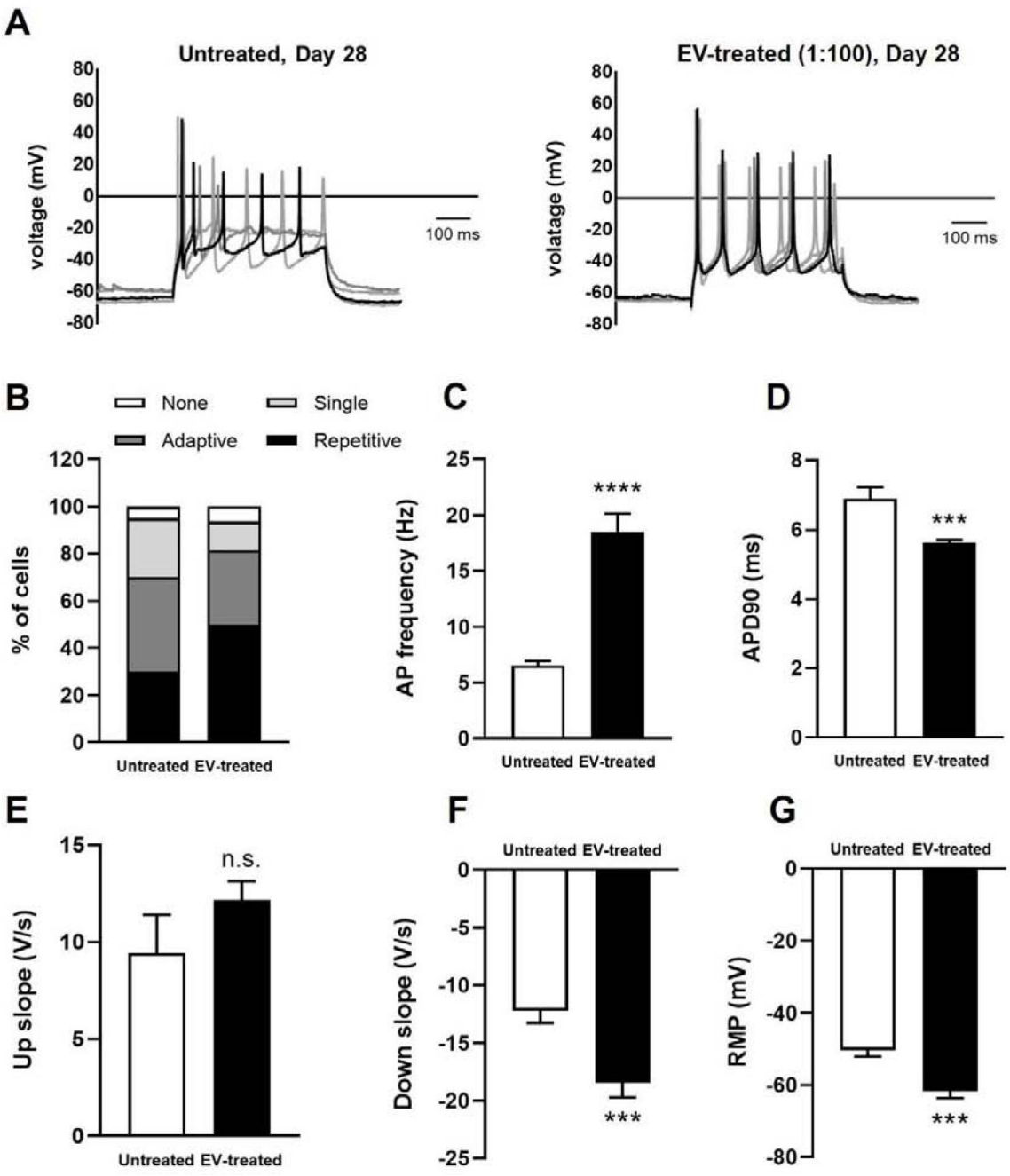

Figure 6. Single cell electrophysiology of EV-treated and untreated neurons.

(A) Representative action potential traces recorded from EV-treated and untreated neurons. (B) Number of patched neurons exhibiting different action potential firing patterns, categorized as ‘repetitive’, ‘adaptive’, ‘single’, and ‘none’. A contingency table comparing EV treatment condition against firing behavior found that the two factors are significantly related ($p = 0.018$), suggesting that the frequency of firing type occurrence is dependent on the presence or absence of EVs in the culture medium. (C) Maximum action potential firing rate in each group of neurons measured in response to a 500 ms depolarizing current injection. (D) The action potential duration at 90% of repolarization (APD90).

Depolarization speed (E) and repolarization speed (F) of neurons relative to the apex of the recorded action potential. (G) Resting membrane potential measured from unstimulated neurons with 0 pA current injection. In all presented data, error bars represent standard error of the mean, and ***$p<0.0003$ ****$p<0.0001$, ns not significant. n = 20 (untreated), n = 16 (EV-treated) for each data set.

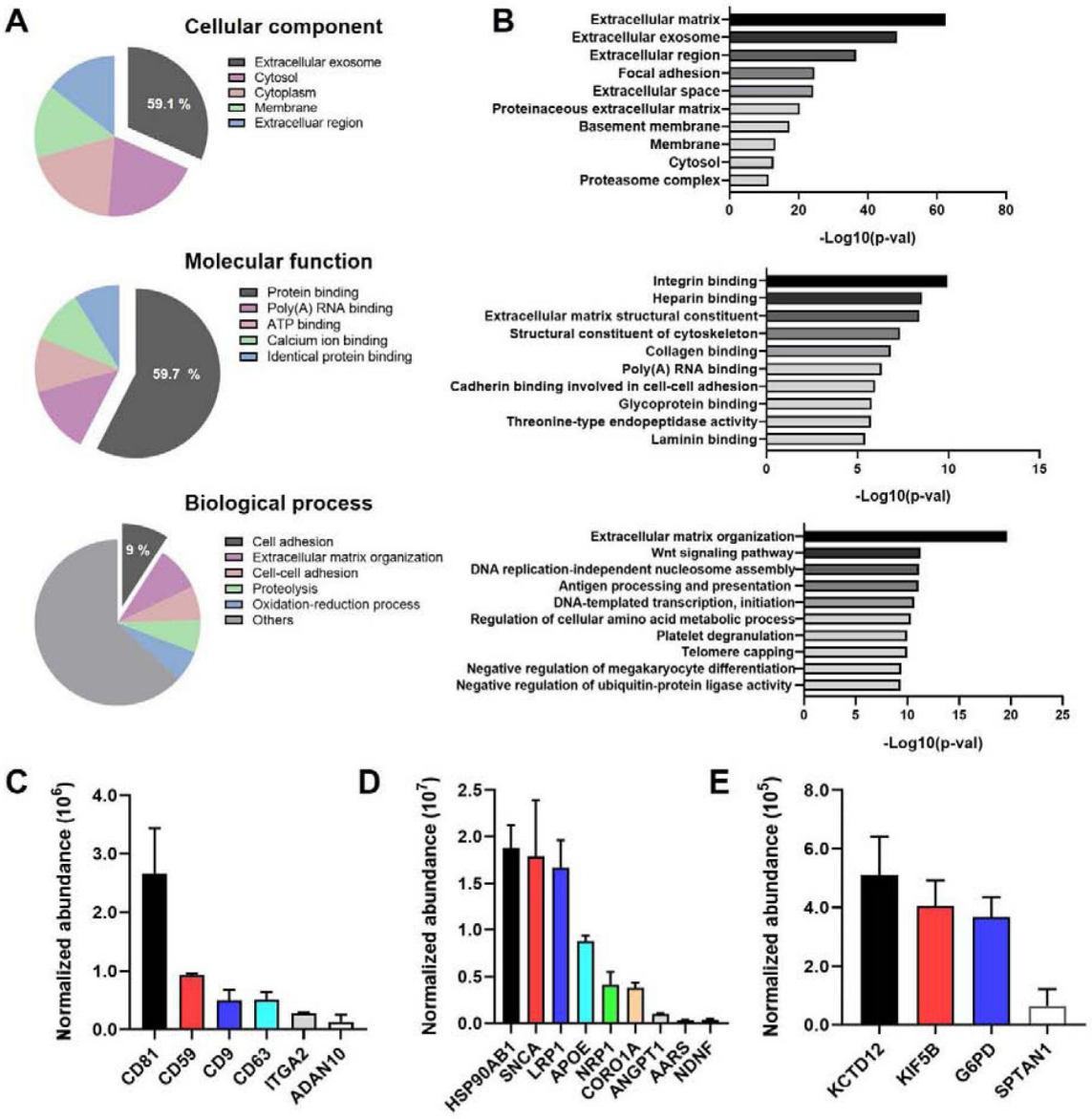

Figure 7. Proteomics analysis of astrocyte-derived EVs.

Top 5 GO terms ordered by protein % for the following categories: cellular component (A), molecular function (A-1) and biological process (A-2). (B) The most enriched GO terms for each of the GO categories using the normal EV cargo protein list as a background.[60] (C) Normalized abundance of astrocyte-EV membrane proteins discovered. The most up-to-date list of EV surface proteins as a reference is obtained from literature.[24] (D) Normalized abundances of astrocyte-EV proteins involved in the negative regulation of neuronal apoptosis. (E) Normalized abundances of astrocyte-EV proteins that may be involved in neuronal ion channel and membrane excitability modulation. In all presented data, error bars represent the standard deviation.